Intramolecular Dephosphorylation of ERK by MKP3†

Youngjoo Kim,‡ Adrian E. Rice,‡ and John M. Denu*,§

University of Wisconsin−Madison, Department of Biomolecular Chemistry, Madison, Wisconsin 53706, and Oregon Health and Science University, Department of Biochemistry and Molecular Biology, Portland, Oregon 97239-3098

Received July 29, 2003; Revised Manuscript Received October 23, 2003

ABSTRACT: The dual specificity mitogen-activated protein kinase phosphatase MKP3 downregulates mitogenic signaling through dephosphorylation of extracellular signal-regulated kinase (ERK). Like other MKPs, MKP3 consists of a noncatalytic N-terminal domain and a catalytic C-terminal domain. ERK binding to the N-terminal noncatalytic domain of MKP3 has been shown to increase (up to 100-fold) the catalytic activity of MKP3 toward small artificial substrates. Here, we address the function of the N-terminal domain of MKP3 in either inter- or intramolecular dephosphorylation of pERK (phosphorylated ERK) and the stoichiometry of the MKP3/pERK Michaelis complex. These are important mechanistic distinctions given the observation that ERK exists in a monomer/dimer equilibrium that is shifted toward the dimer when phosphorylated and given that MKP3 undergoes catalytic activation toward other substrates when bound to ERK. Wild-type and engineered mutants of ERK and MKP3, binding analyses, reaction kinetics, and chemical cross-linking studies were used to demonstrate that the monomer of MKP3 binds to the monomeric form of pERK and that MKP3 within the resulting heterodimer performs intramolecular dephosphorylation of pERK. This study provides the first direct evidence that MKP3 utilizes intramolecular dephosphorylation between a complex consisting of one molecule each of MKP3 and ERK. Catalytic activation and substrate tethering by MKP3 lead to a ≥4000-fold rate enhancement (k_{cat}/K_m) for dephosphorylation of pERK.

Protein phosphorylation is one of the most fundamental regulatory mechanisms in living cells, and it is controlled by the opposing actions of protein kinases and phosphatases. Protein kinases referred to as the mitogen-activated protein (MAP)[1] kinases are critical components in cellular signaling. The MAP kinase family comprises three structurally and functionally distinct enzyme classes: the extracellular signal-regulated kinases (ERK), c-Jun NH_2-terminal kinase/stress-activated protein kinase (JNK/SAPK), and p38/RK/CSBP (p38) (*1*−*3*). Full activation of the MAP kinases requires phosphorylation on both threonine and tyrosine residues in the TXY motif (*4*). Activated MAP kinases phosphorylate key regulatory proteins and transcription factors, leading to their activation. These activated MAP kinases are the targets for some dual-specificity phosphatases (DSPs). Since specific DSPs have been shown to inactivate MAP kinases (*5*−*8*), many have been coined MAP kinase phosphatases (MKPs). Compared with protein tyrosine phosphatases (PTPs), which share the active-site motif HCxxGxxR(S/T), DSPs can be distinguished by their ability to hydrolyze all three major phosphorylated residues (phosphotyrosine, phosphothreonine, and phosphoserine). There are 12 distinct mammalian MKPs (*9*, *10*) that have similar structural domains composed of an N-terminal noncatalytic domain and a C-terminal catalytic domain where the active-site motif, HCxxGxxR(S/T), is located. The amino-terminal domain has two short-sequence motifs (CH2A and CH2B) that display low homology to regions within the catalytic domain of the Cdc25 phosphatase (*10*, *11*). Studies have shown that several MKPs display distinct in vivo substrate preferences for the various MAP kinases (*5*, *12*−*14*). For example, it has been shown that MKP3 selectively targets ERK (*5*), while M3/6 (hVH-5) shows a preference for JNK and p38 (*12*). Recently, SKRP1 (SAPK pathway-regulating phosphatase 1) was shown to inactivate the JNK pathway (*15*).

Several of these MKPs exhibit catalytic activation when bound to their reported kinase substrates (*16*−*19*). In particular, MKP3 is a poor enzyme toward small phosphoesters such as para-nitrophenyl phosphate (*p*NPP). However, in the presence of ERK, the catalytic activity of MKP3 increases >35-fold toward *p*NPP (*16*, *20*, *21*). It has been shown that this dramatic increase in MKP3 phosphatase activity toward synthetic substrates is mediated by the tight binding of ERK to the N-terminal domain of MKP3 (*16*, *20*, *21*, *32*). Activation is due to the ability of ERK to stabilize the active conformer of the catalytic domain through closure of the general acid loop (*20*, *21*). Positively charged amino acid clusters in the N-terminal domain of MKP3 have been shown to be required for the docking of ERK through negatively charged aspartic acid residues (*22*). It has also been suggested that the N-terminal domain of MKP3, as well

† This work was supported by NIH Grant GM59785 to J.M.D. and American Heart Association Predoctoral Fellowship to Y.K.

* Corresponding author. Phone: (608) 265-1859. Fax: (608) 262-5253. E-mail: jmdenu@wisc.edu.

‡ Oregon Health and Science University.

§ University of Wisconsin−Madison.

[1] Abbreviations: MAP, mitogen-activated protein; ERK, extracellular signal-regulated protein kinase; MEK, mitogen-activated protein kinase/extracellular signal-regulated protein kinase kinase; MKP, mitogen-activated protein kinase phosphatase; *p*NPP, para-nitrophenyl phosphate; DSP, dual-specificity phosphatase; PTPase, protein tyrosine phosphatase; VHR, *vaccinia H1*-related.

10.1021/bi035346b CCC: $25.00
Published on Web 11/26/2003

as other MKPs, contribute to the substrate specificity observed toward various MAP kinase members (*23*, *24*, *33*). Although most detailed mechanistic evaluations of MKP3 have been done using the artificial substrate *p*NPP, few studies have been directed at understanding the dephosphorylation mechanism of its authentic substrate, pERK (phosphorylated ERK at residues threonine 183 and tyrosine 185). Recently, Zhao et al. (*23*) demonstrated that the catalytic efficiency of MPK3 for pERK was 6 orders of magnitude higher than that of the MKP3-catalyzed *p*NPP hydrolysis, due to the reported low K_m for pERK (~20 nM) (*23*).

Two important questions concerning the dephosphorylation mechanism remain unresolved. Does MKP3 catalyze intra- or intermolecular dephosphorylation of pERK? What is the stoichiometry of the relevant MKP3/ERK complex? ERK is known to exist in equilibrium between monomeric and dimeric forms, which are shifted toward the dimeric form upon phosphorylation by its upstream kinase. ERK dimerization has been proposed as a requisite for nuclear translocation and function. The oligomeric state of MKP3 is not known, although MKP3 undergoes catalytic activation toward other substrates when bound to ERK. These observations suggest that MKP3 could be activated by one molecule of ERK while it dephosphorylates a separate molecule, either free in solution or within an ERK dimer. Alternatively, MKP3 may dephosphorylate the same ERK molecule to which it is bound through the N-terminus of MKP3. In this study, we address these questions by examining the role of the N-terminal domain of MKP3, whether the reaction is catalyzed via inter- or intramolecular dephosphorylation of pERK, and the stoichiometry of the MKP3/pERK Michaelis complex.

MATERIALS AND METHODS

Protein Preparation. MKP3 (*24*), VHR (*25*), and ERK (*26*) were expressed and purified as described previously. The MKP3/VHR chimera was generated by fusing the N-terminal domain of MKP3 to VHR using a PCR method. The fusion cDNA was generated using our existing pT7-VHR (*25*) and pT7-MKP3 His_{x6} expression vector (*24*) by standard PCR methods. The PCR fragment containing the VHR catalytic domain was inserted into pT7-MKP3, replacing the catalytic domain of MKP3. MKP3 and VHR were fused through the identical amino acid sequence SDGS. The SDGS sequence in VHR (17−20 in 185 residues VHR) is found in the loop between the first α-helix and first β-strand (*27*). In MKP3, SDGS resides in the N-terminal domain close to the catalytic domain (193−196 in 381 residue protein; catalytic domain starts at 204 amino acid residue). The MKP3/VHR chimera was expressed and purified as described for MKP3 (*24*). D316/319N ERK was generated by single oligonucleotide site-directed mutagenesis, as described previously (*28*), and expressed and purified as described for wild-type ERK (*26*). The expression vector for L4A H176E ERK (GST (glutathione-*S*-transferase) tagged at the N-terminus and His_{x6}-tagged at the C-terminus) was a generous gift from M. Cobb (University of Texas, Southwestern Medical Center, Dallas, TX) (*29*). L4A H176E ERK was expressed as described for wild-type ERK (*26*). The bacterial lysate was incubated with glutathione-agarose resin (Sigma) for 30 min at 4 °C. The resin was washed with ERK buffer (50 mM sodium phosphate, 300 mM NaCl, l0 mM β-mercaptoethanol) and incubated with thrombin (Sigma) for 1 h at 25 °C to cleave the GST from L4A H176E ERK. Flow-through containing L4A H176E ERK was collected and separated from thrombin using Ni^{2+}-NTA agarose (Qiagen). L4A H176E ERK was batch eluted with 300 mM imidazole and quantitated by SDS−PAGE. Phosphorylated L4A H176E ERK was able to phosphorylate myelin basic protein (MBP) with similar efficiency to that of wild-type pERK, indicating that these mutations do not alter the function and overall structure of the kinase. All the proteins were aliquoted and stored at −80 °C. Phosphorylation of recombinant rat wild-type and mutant ERK2 proteins was performed as described previously (*30*).

pNPP Assays. The assay buffer consisted of a three-component system containing 0.1 M acetate, 0.05 M Tris, and 0.05 M bis-Tris. To determine the kinetic parameters k_{cat}, K_m, and k_{cat}/K_m, the initial velocities were measured at increasing substrate concentrations. The apparent second-order rate constant k_{cat}/K_m describes the reaction between free enzyme and free substrate. The reactions were quenched with 10 N NaOH, and the production of *p*NP (para-nitrophenolate) was measured using a Multiskan Ascent microplate reader (Lab Systems) at 405 nm. The data were fitted to the Michaelis−Menten equation using software Kaleidagraph (Abelbeck Software) (eq 1).

$$v = [E_0]k_{cat}S/(S + K_m) \quad (1)$$

Generation of MKP3 Antibody. Chicken immunopurified anti-MKP3 antibody was generated by immunizing chickens with the full-length MKP3 protein. The IgY fraction was purified from egg yolks (Aves Labs). MKP3 antibody was purified over a column containing recombinant MKP3 conjugated to Affi-Gel 10 (Sigma). Chicken antibodies were eluted with 0.1 M sodium phosphate (pH 2.5) and stored in phosphate-buffered saline (PBS).

Dephosphorylation of Recombinant ERK2 Proteins by Phosphatases. Recombinant MKP3, VHR, and the MKP3/VHR chimera were combined with 1 μM recombinant phosphorylated ERK2 proteins (wild-type, D316/319N, and L4A H176E) in 0.1 M sodium acetate, 0.05 M Tris, and 0.05 M bis-Tris (TBA) (pH 7.0 for MKP3 and pH 6.0 for VHR and MKP3/VHR Chimera) and incubated up to 1 h at 25 °C. Aliquots were withdrawn at the indicated times and added to the tubes containing 5x Laemmli sample buffer to terminate the reactions. The samples were then subjected to Western blot analysis as described previously to examine the phosphorylation state of ERK2 using an antibody specific to phosphorylated forms of p44/42 MAPK (Thr^{202}/Tyr^{204}) (New England Biolabs) (*31*). Changes in the phosphorylation state of the ERK proteins were quantified by densitometry using a Bio-Rad GS-700 Imaging Densitometer and the Molecular Analyst Software (Bio-Rad). The identical samples were also coupled to a kinase assay to directly examine the effect of phosphatases on the activity of phosphorylated ERK as described previously (*31*). The amount of dephosphorylated ERK proteins was determined by subtracting the fraction remaining from one and multiplying by the initial concentration of phosphorylated ERK proteins. The data were fitted to the integrated Michaelis−Menten equation (eq 2) using software Kaleidagraph (Abelbeck Software) to obtain apparent second-order rate constant k_{cat}/K_m.

$$t = p/k_{cat}E_0 + [K_m/k_{cat}E_0] \ln[p\infty/p\infty - p] \quad (2)$$

where E_0 is the enzyme concentration, $p\infty$ is the product concentration upon complete reaction, and p is the product concentration at time t. For the dephosphorylation of pERK by the MKP3 and MKP3/VHR chimera, eq 2 was modified to eq 3. After MKP3 dephosphorylates pERK, the product (unphosphorylated ERK) builds up and binds to the N-terminal domain of MKP3 and inhibits the binding of the pERK substrate. Therefore, we included an inhibition constant term in eq 2 and fitted the data using eq 3 (*25*).

$$t = p/k_{cat}E_0 + [(1 + (p/K_i))K_m/k_{cat}E_0] \ln[p\infty/p\infty - p] \quad (3)$$

where E_0 is the enzyme concentration, $p\infty$ is the product concentration upon complete reaction, p is the product concentration at time t, and K_i is the inhibition constant for ERK. We used 0.21 and 0.23 μM for the K_i for the MKP3 and MKP3/VHR chimera, respectively (described in the text).

Fluorescent Anisotropy. Wild-type ERK and D316/319N ERK (120 μM) were labeled with fluorescein succinimidyl ester (5 mM) using a Fluorescein Amine Labeling Kit (Pan Vera, WI). Stoichiometry of labeling was 0.86 fluorescein succinimidyl ester per ERK monomer. The labeled proteins (30 nM) were titrated with either MKP3 or MKP3/VHR chimera (0−1.6 μM). The changes in millipolarization were measured using a fluorescent anisotropy instrument (Pan Vera, WI). The total differential fluorescent polarization signal was 15∼20 mP. Percent bound of labeled ERK proteins was plotted versus the free MKP3 concentrations, and data were fitted to eq 4.

$$[ERK{\cdot}MKP3] = ([ERK]_0[MKP3]_{free})/(K_d + [MKP3]_{free}) \quad (4)$$

The MKP3 concentration that is bound to ERK was calculated by multiplying the concentration of ERK to fractions of bound ERK. Free MKP3 concentrations were determined by subtracting the bound MKP3 concentration from the total MKP3 concentration.

Chemical Cross-Linking of C293S MKP3 and pERK. To assess the oligomeric state of the MKP3 and ERK complex, the proteins were cross-linked with glutaraldehyde. The reactions were performed in 100 μL solutions containing 8 μM C293S MKP3, pERK, or the 1:1 mixture of C293S MKP3 and pERK in 20 mM Tris·Cl (pH 7.5) at 25 °C. Cross-linking was initiated by adding glutaraldehyde to a final concentration of 5 mM. The cross-linking reactions were terminated at various time points (0−40 min) by adding glycine (pH 9.0) at a final concentration of 0.2 M. The cross-linked proteins were subjected to SDS−PAGE and detected by either Coomasie staining or Western blot analysis using chicken-polyclonal antibody specific to MKP3 and rabbit-polyclonal antibody specific to phosphorylated ERK.

Dissociation Constant of D316/319N ERK and L4A H176E ERK to MKP3. The initial rates of *p*NPP hydrolysis in the presence of increasing concentrations of ERK proteins were measured spectrophotometrically at 405 nm. The k_{cat}/K_m values at different concentrations of ERK proteins were determined by measuring the initial velocities at increasing substrate concentrations (0−2 μM) and fitting the data to eq 1. To obtain the amount of bound ERK, $(k_{cat}/K_m)/(k_{cat}/K_m)_{max}$ was multiplied by the concentration of MKP3. The bound ERK concentrations were plotted against the free ERK concentration, and the data were fitted to eq 4 to obtain the dissociation constant of ERK binding to MKP3.

RESULTS

N-Terminal Domain of MKP3 Increases the Effective pERK Substrate Concentration. Initially, we addressed the role of the N-terminal domain of MKP3 in mediating either intra- or intermolecular dephosphorylation of pERK. To accomplish this, it was necessary to separate the catalytic activation from the evaluation of the catalytic advantage between intramolecular and intermolecular dephosphorylation. We generated a chimeric protein where the catalytic domain of MKP3 was replaced with the catalytic domain of human VHR (*vaccinia H1*-related). VHR represents the minimal, naturally occurring catalytic domain among dual-specificity phosphatases. pERK has been previously identified as an in vivo and in vitro substrate of VHR (*31*, *34*). However, VHR does not contain the N-terminal domain of the MKPs and does not require catalytic activation, as it is fully active toward a variety of phospho-monoester substrates. We investigated the effect of fusing the N-terminal domain of MKP3 onto the catalytic domain of VHR. Generation of the chimeric protein is detailed in the Materials and Methods. We first measured the steady-state kinetic parameters (k_{cat}, K_m, k_{cat}/K_m) of MKP3, VHR, and the MKP3/VHR chimera using *p*NPP as a substrate. The MKP3/VHR chimera displayed catalytic efficiencies that were similar to those of wild-type VHR using *p*NPP as a substrate (Table 1). The k_{cat} value of the MKP3/VHR chimera was only 2.7-fold lower than that of VHR, whereas the K_m value was nearly identical. Because MKP3 can be activated by ERK binding to the N-terminal domain (refs *20*, *21*, and *32* and Table 1), we examined whether the catalytic activity of the MKP3/VHR chimera can be further activated by ERK binding. The addition of ERK in the reaction had no significant effect on the steady-state kinetic parameters of either the MKP3/VHR chimera or VHR, using *p*NPP as a substrate (Table 1), consistent with constitutively active enzymes that do not require ERK binding for activation. These results demonstrate that we have successfully eliminated the catalytic activation step as a necessary component for efficient dephosphorylation by the MKP3/VHR chimera, allowing us to now evaluate the direct contribution of the N-terminal domain toward either inter- or intramolecular dephosphorylation of ERK.

However, we could not rule out the possibility that the MKP3/VHR chimera was incapable of binding ERK. To be certain that ERK binds to the N-terminal domain of the MKP3/VHR chimera, binding assays were performed using a fluorescent anisotropy method. ERK and a D316/319N ERK mutant were labeled with fluorescein as described in the Materials and Methods. The labeled ERK proteins, at a concentration of 30 nM, were titrated with 0−1.6 μM MKP3 or MKP3/VHR chimera. The change in millipolarization was measured and plotted against the free phosphatase concentration, and the titration curves were fitted to eq 4 (Figure 1). The D316/319N ERK mutant served as a negative control for establishing this binding method. These aspartic acid residues in ERK have been shown to be critical for binding to the N-terminal domain of MKP3 (*22*). Additional control experiments were performed to establish that labeling

Table 1: *p*NPP Hydrolysis Activity by VHR, MKP3/VHR Chimera, and Wild-Type MKP3, pH 6.0 at 25 °C[a]

	VHR	VHR + ERK	chimera	chimera + ERK	MKP3	MKP3 + ERK
k_{cat} (s^{-1})	6.20 ± 0.43	6.25 ± 0.23	2.30 ± 0.12	2.84 ± 0.11	0.024 ± 0.005	0.45 ± 0.08
K_m (mM)	2.17 ± 0.42	2.32 ± 0.31	3.25 ± 0.41	2.30 ± 0.25	5.12 ± 1.01	1.5 ± 0.14
k_{cat}/K_m (M^{-1} s^{-1})	2863 ± 390.4	2694 ± 252	742 ± 59.4	1235 ± 91.0	4.69 ± 1.34	305 ± 78.5

[a] The initial velocities were measured using 100 nM enzymes at increasing substrate concentrations (0−20 mM) to determine the kinetic parameters k_{cat}, K_m, and k_{cat}/K_m. ERK was added as a 2-fold excess to the enzymes (200 nM). The reactions were quenched with 10 N NaOH, and the production of *p*NP (para-nitrophenolate) was measured using a Multiskan Ascent microplate reader (Lab Systems) at 405 nm. The data were fitted to the Michaelis−Menten equation using the software Kaleidagraph (Abelbeck Software). $v = [E_0]k_{cat}S/(S + K_m)$. The values are averaged from three separate experiments.

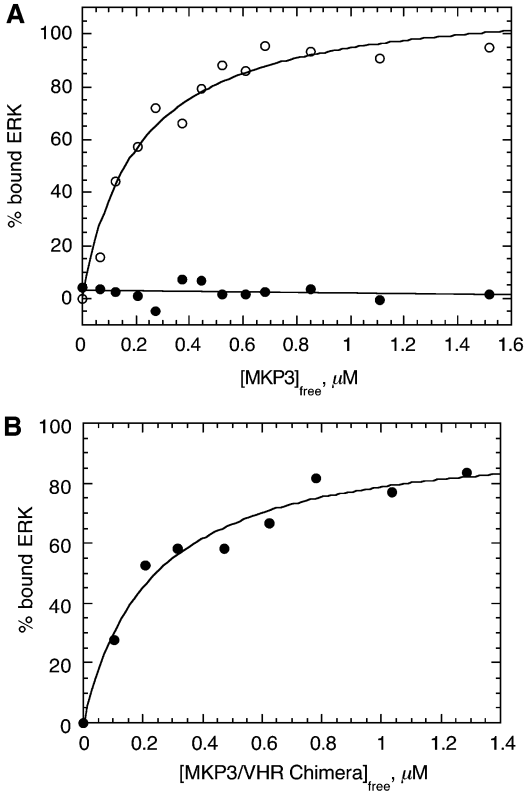

FIGURE 1: Binding affinity of ERK to MKP3 and an MKP3/VHR chimera. Wild-type ERK and D316/319N ERK were labeled with fluorescein as described in the Materials and Methods. The labeled enzymes (30 nM) were titrated with 0−1.6 μM MKP3 (panel A, open circles) or MKP3/VHR Chimera (panel B, filled circles). Binding data for the D316/319N ERK mutant are shown in panel A, filled circles. The changes in millipolarization were measured using a fluorescent anisotropy instrument and plotted against phosphatase concentrations. Percent bound of labeled proteins was plotted vs free MKP3 concentrations, and data were fitted to eq 4 using Kaleidagraph. The binding constants for ERK to the wild-type MKP3 and the MKP3/VHR chimera were 0.21 ± 0.04 and 0.23 ± 0.05 μM, respectively. These values are an average of three separate experiments.

(~1:1, fluorescein to ERK monomer) had no affect on the ability to bind MKP3 (Supporting Information, Figure 1). The dissociation constants (K_d) for ERK binding to the wild-type MKP3 (Figure 1A) and the MKP3/VHR chimera (Figure 1B) were 0.21 ± 0.04 and 0.23 ± 0.05 μM, respectively. These values were identical within experimental error. The K_d of MKP3 for ERK was similar to the value (0.17 μM) reported by Zhou et al. (*35*). No measurable binding of the D316/319N ERK mutant was observed under identical conditions (Figure 1A). Our data indicate that ERK binds to both MKP3 and the MKP3/VHR chimera with similar affinity; however, binding does not cause an increase

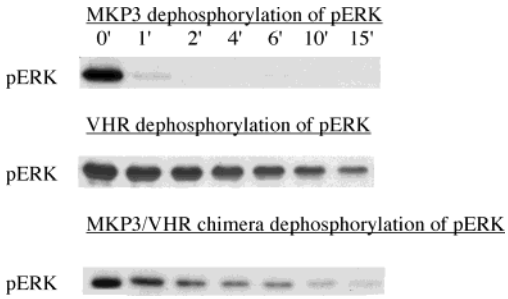

FIGURE 2: Time-dependent dephosphorylation of pERK by MKP3, VHR, and an MKP3/VHRchimera. MKP3, VHR, and the MKP3/VHR chimera (100 nM) were incubated with phosphorylated ERK (1 μM) at 25 °C for 0−15 min (TBA, pH 6.0 for VHR and MKP3/VHR chimera, pH 7.0 for MKP3). Dephosphorylation of pERK was determined by Western blot analysis using antibodies specific to the dually phosphorylated form of ERK, and the data were fitted to the integrated Michaelis−Menten equation (eq 2) as described in the Materials and Methods. For the MKP3 and MKP3/VHR chimera, the inhibition constants were taken into account as in eq 3.

in the catalytic activity of the MKP3/VHR chimera. Like VHR, the MKP3/VHR chimera appears to be in a constitutively active state where ERK binding to the N-terminal domain does not further activate the enzyme toward small artificial substrates, like *p*NPP.

Having established that the chimera does not exhibit catalytic activation when bound to ERK, next we compared the catalytic activity of MKP3, VHR, and the MKP3/VHR chimera toward an authentic protein substrate, pERK. Recombinant MKP3, VHR, and the MKP3/VHR chimera, at a final concentration of 100 nM, were combined with 1 μM recombinant pERK. Dephosphorylation was detected by Western blot analysis using an antibody that specifically recognizes the diphosphorylated active form of ERK (a representative data set is shown in Figure 2). The bands were quantitated by densitometry, and the data were fitted to the integrated Michaelis−Menten equation (eqs 2 or 3) as described in the Materials and Methods. The k_{cat}/K_m values for pERK dephosphorylation by MKP3, VHR, and the MKP3/VHR chimera were 3.1 ± 1.9 × 10^6, 20 530 ± 1300, and 1.1 ± 0.23 × 10^6 M^{-1} s^{-1}, respectively. These values are an average of three or more separate experiments. The Western blot analysis of pERK dephosphorylation was confirmed with a separate kinase assay as described in the Materials and Methods. The k_{cat}/K_m values for pERK dephosphorylation by VHR and the MKP3/VHR chimera using the kinase assay were 9750 ± 923 and 0.40 ± 0.12 × 10^6 M^{-1} s^{-1}, respectively (see Supporting Information, Figure 2). These values are in reasonable agreement with the values obtained from the Western blot analysis. Quite dramatically, the MKP3/VHR chimera was a more efficient enzyme

(~ 40-fold higher in k_{cat}/K_m) than wild-type VHR in dephosphorylating pERK. This suggests that the N-terminal domain of MKP3 is contributing significantly to enhance catalysis of pERK through specific binding to the N-terminal domain. Since we have shown that the MKP3/VHR chimera was not catalytically activated by ERK binding (Table 1), the increased k_{cat}/K_m value over wild-type VHR is likely the result of an increase in the effective concentration of pERK. Although the chimera is an engineered enzyme, the fact that it exhibits gain of function behavior provides evidence for an intramolecular dephosphorylation mechanism of pERK by MKP3. The catalytic advantage of an increase in effective substrate concentration would be realized when the substrate and enzyme are tethered within the same complex.

Intramolecular Dephosphorylation of pERK by MKP3. To investigate whether pERK inactivation by MKP3 proceeds by intramolecular or intermolecular dephosphorylation, we next examined the mechanism by which unphosphorylated ERK inhibits pERK dephosphorylation. If the reaction is intramolecular and involves MKP3 dephosphorylating the same pERK molecule to which its N-terminal domain is bound, then excess unphosphorylated ERK should inhibit dephosphorylation by competing with pERK at the N-terminus and blocking an intramolecular reaction. Consistent with this, Zhao et al. (*23*) recently showed that unphosphorylated ERK acted as a classical competitive inhibitor of pERK dephosphorylation by MKP3. However, the basis for the observed inhibition was not established since an excess amount of unphosphorylated ERK in the reaction could block the reaction by either binding the N-terminal domain, the catalytic domain, or both.

Consistent with the results of Zhao et al (*23*), we demonstrate that excess unphosphorylated ERK (10 μM) can readily inhibit pERK (1 μM) dephosphorylation by MKP3 (Figure 3A). To investigate whether this inhibition was due to competition for binding at the N-terminal domain, we took advantage of a *Sevenmaker* type of mutant ERK (*36*), where we mutated two aspartic acid residues to asparagine residues (D316/319N ERK). These aspartic acid residues form negative clusters in ERK and have been shown to be critical for binding to the N-terminal domain of MKP3 (*22*). Once expressed and purified, we verified that D316/319N ERK does not bind tightly to the N-terminal domain of MKP3 by determining the ability of D316/319N ERK to activate MKP3 against the *p*NPP substrate. There was minimal catalytic activation of MKP3 toward *p*NPP in the presence of D316/319N ERK at a 5-fold molar excess (Figure 3B). In positive control experiments, MKP3 was activated approximately 50-fold when wild-type ERK, at 2-fold molar excess, was present in the assay. In an effort to measure a dissociation constant of D316/319N ERK binding to MKP3, the initial rates of *p*NPP hydrolysis in the presence of increasing levels of D316/319N ERK were measured and analyzed as described in the Materials and Methods. Given the lack of significant binding, the estimated K_d with D316/319N ERK was >10 μM (data not shown), suggesting that D316/319N ERK exhibits greatly diminished binding to the N-terminal domain of MKP3, consistent with the fluorescence polarization binding data of Figure 1A. To verify that the D316/319N ERK mutant is structurally intact, the mutant was phosphorylated in vitro with its upstream kinase MEK, and the ability of the activated kinase D316/319N pERK to phosphorylate myelin basic protein was compared to wild-type pERK. Similar activities were observed (data not shown), suggesting that the double mutant D316/319N ERK is structurally and functionally intact and that the loss of

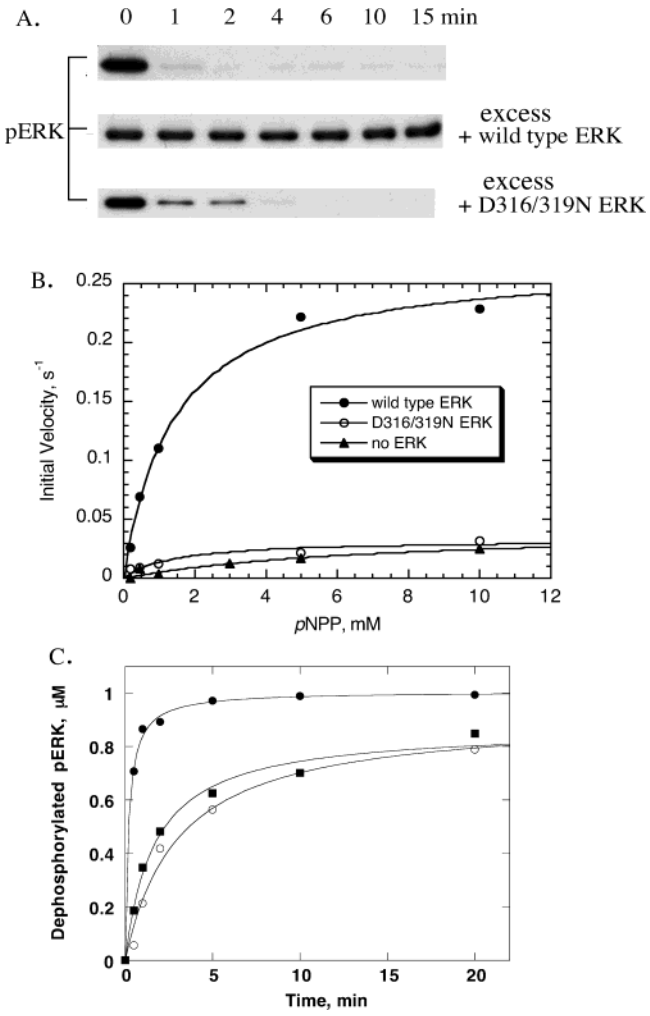

FIGURE 3: Unphosphorylated ERK competes with phosphorylated ERK for binding at the N-terminal domain of MKP3. (A) Time-dependent dephosphorylation of pERK by MKP3. MKP3 (100 nM) was incubated with phosphorylated ERK (1 μM) at 25 °C for 0−15 min (TBA, pH 7.0). Dephosphorylation of pERK was determined by Western blot analysis using antibodies specific to the diphosphorylated form of ERK. For the dephosphorylation of pERK in the presence of unphosphorylated ERK (wild-type and D316/319N), 10 μM unphosphorylated ERK was preincubated with 100 nM MKP3 for 5 min at 25 °C, and then reactions were initiated by adding pERK to the preincubated MKP3-ERK complex. (B) The catalytic activation of MKP3 in the presence of ERK or D316/319N ERK. The 0.28 μM MKP3 was incubated with 0.60 μM of either wild-type ERK or D316/319N ERK. The phosphatase substrate *p*NPP, ranging from 0 to 10 mM, was used to examine the effect of ERK on the phosphatase activity of MKP3 (TBA, pH 7.0). The data were fitted using the Michaelis−Menten equation (eq 1). The D316/319N ERK double mutant did not activate MKP3. The graph is an average of three separate experiments. (C) Time-dependent ERK dephosphorylation by MKP3 and inhibition in the presence of unphosphorylated ERK or the L4A H176E mutant. Data were generated and analyzed as in panel A. MKP3 (100 nM) was incubated with phosphorylated ERK (1 μM) at 25 °C for 0−20 min (filled circles). Open circles represent pERK dephosphorylation in the presence of 10 μM unphosphorylated ERK, and the filled squares represent pERK dephosphorylation in the presence of 10 μM unphosphorylated L4A H176E mutant. The graph represents an average of two separate experiments.

MKP3 binding reflects specific alterations in the binding interface.

In competition experiments similar to those described for wild-type enzyme (Figure 3A), excess D316/319N ERK exhibited only a very small inhibitory effect on the ability of MKP3 to dephosphorylate wild-type pERK (Figure 3A), which is likely due to some residual binding of D316/319N ERK to MKP3. These data provide strong support for the idea that the inhibition of pERK dephosphorylation by native ERK was due to ERK binding to the N-terminal domain of MKP3 and not due to competition at the active site of MKP3. Moreover, these data are consistent with an intramolecular dephosphorylation mechanism where pERK has to bind to the N-terminal domain of MKP3 to be effectively dephosphorylated by the catalytic domain of the same MKP3 molecule; however, the possibility existed that inhibition of pERK dephosphorylation in the presence of excess ERK might be due to dimerization between pERK and unphosphorylated ERK, leading to a depletion of monomeric pERK as a substrate for MKP3, if the monomeric form is the relevant substrate. To rule out this possibility, we performed pERK dephosphorylation reactions in the presence of an excess of a dimerization mutant of ERK (L4A H176E), where four leucine residues (L333, 336, 341, 344) are mutated to alanine and one histidine residue is changed to glutamic acid. These residues have been shown to be important in ERK dimerization upon phosphorylation (*29*). We observed similarly inhibited rates of pERK dephosphorylation by MKP3 in the presence of the same concentration of either excess wild-type ERK or dimerization mutant ERK (Figure 3C). These data rule out mixed ERK dimerization as the source of inhibition and demonstrate that the observed inhibition by unphosphorylated ERK is derived from direct competition between pERK for the N-terminal domain of MKP3.

To further distinguish between inter- and intramolecular dephosphorylation, we analyzed the ability of MKP3 to hydrolyze the phosphorylated form of the D316/319N ERK mutant under a variety of conditions where MKP3 is utilized in the basally active state (MKP3 alone) or the activated state (MKP3 bound to unphosphorylated wild-type ERK). Because D316/319N ERK does not bind tightly to MKP3, this mutant cannot activate MKP3 under the conditions employed. Therefore, dephosphorylation of D316/319N pERK by MKP3 should be greatly diminished. However, the efficiency of D316/319N pERK dephosphorylation by activated MKP3 (ERK-bound form) would depend on whether MKP3 performs inter- or intramolecular dephosphorylation. If MKP3 utilizes an intermolecular mechanism, the activated form of MKP3 (ERK-bound) should be able to efficiently dephosphorylate D316/319N pERK, as there would be no additional requirement to bind to the N-terminal domain of MKP3, only to the catalytic domain. Alternatively, if MKP3 catalyzes intramolecular dephosphorylation, activated or basal MKP3 would not be able to efficiently dephosphorylate D316/319N pERK because of the inability to bind to the N-terminal domain of MKP3. To distinguish between these two mechanisms, we compared k_{cat}/K_m values of wild-type pERK and D316/319N pERK dephosphorylation by MKP3 (both basal state and ERK-bound activated state). As shown in Figure 4, the k_{cat}/K_m values with D316/319N pERK by both the basal and the activated state of MKP3 (12 800 $\pm$ 1230 and 13 510 $\pm$ 1443 M^{-1} s^{-1}, respectively) were similar and were ~200-fold lower than that of wild-type pERK dephosphorylation (3.1×10^6 M^{-1} s^{-1}). These data provide additional evidence for an intramolecular dephosphorylation mechanism, where substrate pERK must interact with the N-terminal domain of MKP3 to be dephosphorylated by the catalytic domain of the same molecule of MKP3.

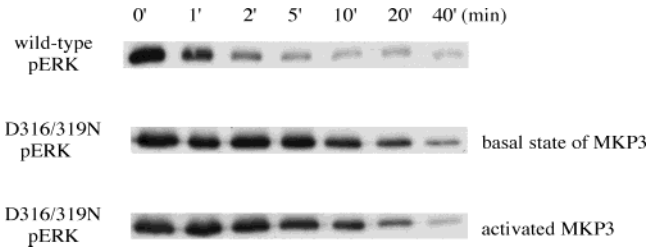

FIGURE 4: Dephosphorylation of wild-type and D316/319N mutant pERK by MKP3. Recombinant wild-type and D316/319N mutant pERK at a final concentration of 1 μM were combined with 0.14 μM recombinant wild-type MKP3 in TBA, pH 7.0. Reactions were incubated at 25 °C for the indicated times prior to quenching. For the pERK dephosphorylation reaction by activated MKP3, MKP3 (0.14 μM) was preincubated with unphosphorylated ERK (0.28 μM) and used for dephosphorylating pERK. The rate of dephosphorylation was measured using the integrated Michaelis−Menten equation including the inhibition constant term (eq 3) as described in the Materials and Methods.

Stoichiometry of the Substrate/Enzyme Complex of pERK-Bound MKP3. ERK exists in a monomer−dimer equilibrium that can be shifted in favor of the dimer upon phosphorylation by its upstream kinase MEK (*29*). In the cytoplasm, dimerization of phosphorylated ERK has been postulated as the trigger for translocation into the nucleus, where pERK can mediate transcriptional activation (*29*, *37*−*39*). MKP3 has been shown to localize exclusively in the cytoplasm (*17*). Thus, MKP3 could encounter either the monomeric or the dimeric form of pERK as the physiologically relevant substrate. To determine the stoichiometry of the pERK/MKP3 Michaelis complex, we used a chemical cross-linking approach. For this study, it was necessary to use the catalytic mutant of MKP3 (C293S, nucleophile cysteine 293 residue was mutated to a serine residue) to prevent dephosphorylation of the complex. This mutant has no detectable phosphatase activity but displayed a similar binding constant (K_d = 0.2 μM) to that of wild-type MKP3 for ERK. Similarly, other PTPs with this mutation are still able to bind their substrates (*31*, *40*−*43*).

MKP3(C293S), pERK, and a 1:1 mixture of MKP3-(C293S) and pERK were subjected to glutaraldehyde cross-linking as described in the Materials and Methods. The proteins were cross-linked at fixed concentrations of glutaraldehyde (5 mM) over time (up to 15 min). The crossed-linked proteins were resolved by SDS−PAGE, and the gels were probed with antibodies against either MKP3 or phosphorylated ERK. Figure 5A,B shows Western blots of representative data from the cross-linking analysis, which was performed no less than three separate times. Cross-linking of MKP3(C293S) alone indicated no significant amount of crossed-linked species prior to 10 min, although faint bands were noticeable after longer periods of cross-linking (Figure 5 and Supporting Information). Strikingly, when MKP3(C293S) was mixed with an equal amount of pERK, an efficiently crossed-linked band whose molecular

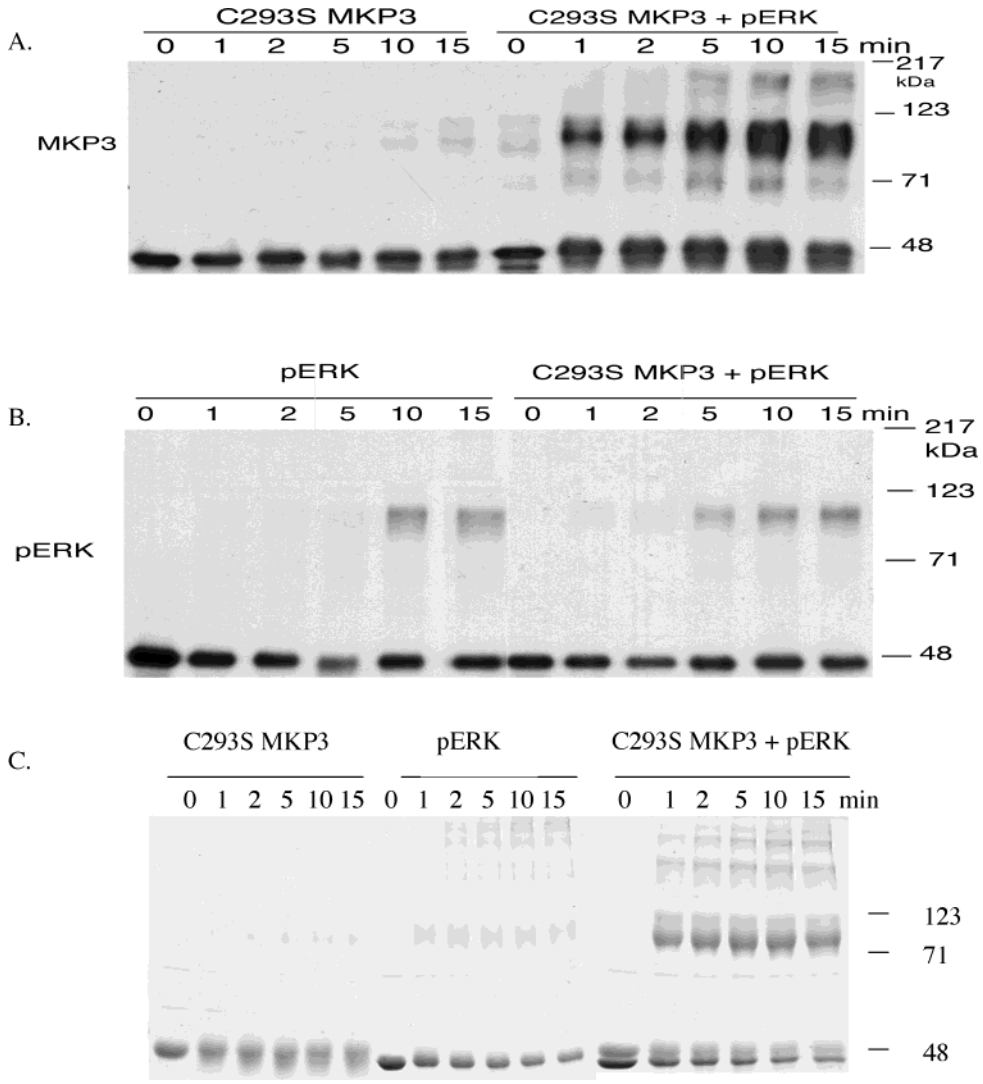

FIGURE 5: Glutaraldehyde cross-linking of C293S MKP3 and pERK. (A and B) MKP3 (8 μM), ERK (8 μM), or a 1:1 mixture of MKP3 and ERK (8 μM each) were cross-linked with 5 mM glutaraldehyde up to 15 min at 25 °C. The reactions were terminated by adding glycine (pH 9.0) at a final concentration of 0.2 mM. The cross-linked species was determined with SDS−PAGE and Western blotting with appropriate antibodies. (C) Coomassie staining of SDS−PAGE of the cross-linked species.

weight (80−90 kDa) corresponds to a heterodimer (predicted 86 kDa) of the two was detected (Figure 5). This major cross-linked band, which was clearly observable after only 1 min, was immunoreactive to both specific antibodies (Figure 5A,B), in agreement with a 1:1 cross link of MKP3 and pERK. Consistent with previous reports that pERK can form a homodimer (*29*), cross-linking of pERK alone yielded a major crossed-linked species at 80−90 kDa.

Because of the fact that both pERK and MKP3 are 43 kDa proteins, crossed-linked species of homodimers and heterodimers exhibited only slight differences in mobility on SDS−PAGE (Supporting Information). However, these cross-linked species could be distinguished by differences in mobility on SDS−PAGE when loaded side by side (Supporting Information).

The Western blot probed with the anti-pERK antibody displayed a much weaker intensity of the cross-linked species than would be expected from the intensity of monomeric pERK (Figure 5A) or from the same band probed with the anti-MKP3 antibody (Figure 5A). To verify that the weaker signal is due to the loss of an epitope upon extensive cross-linking, the cross-linked proteins were detected by Coomassie staining. Using Coomassie detection, most (67%) of the 1:1 protein mixture was cross-linked as the heterodimer under the conditions presented (Figure 5C), suggesting that the Western blot against pERK (Figure 5B) had underrepresented the amount of pERK in the complex. The presence of weak higher oligomers (>dimer) were seen in both the 1:1 mixture and the sample containing only pERK (Figure 5C). Interestingly, as compared with the heterodimer, cross-linking of pERK alone revealed that much of pERK remained monomeric, as relatively small amounts of homodimer were cross-linked (Figure 5C).

Using the identical analysis described previously, we have performed cross-linking studies with unphosphorylated ERK, wildtype MKP3, and a 1:1 mixture of the two (Supporting Information). We found that unphosphorylated ERK and wildtype MKP3 can be efficiently cross-linked to form a similar heterodimer under the conditions used in the previous experiments. In addition to glutaraldehyde, we have used bis[sulfosuccinimidyl]suberate as a cross-linking agent. With ERK and MKP3 alone and in a 1:1 mixture, we observe (by Coomassie staining) no significant cross-linked species with the proteins alone in solution, but we observe a strong

cross-linked band at ~85 kDa in the 1:1 mixture (data not shown), similar to the results we have consistently observed using glutaraldehyde. Nonetheless, we cannot formally discount the possibility that MKP3 can bind dimers of ERK. Significant amounts of larger species (>85 kDa) were not observed. In support of the cross-linking studies, analytical ultracentrifugation experiments indicated that MKP3 existed as a monomeric species (calculated MW of 41 347 kDa of a single ideal component), which when combined with pERK produced a complex consistent with a heterodimer (data not shown).

To provide additional evidence for the idea that MKP3 binds and dephosphorylates the monomeric form of pERK, we utilized the dimerization mutant of ERK (L4A H176E). We investigated the efficiency of MKP3 to dephosphorylate the monomeric form of pERK (L4A H176E pERK). To ensure that the L4A H176E ERK mutant does not display altered binding to MKP3, or diminished ability to activate MKP3, we measured the rate of *p*NPP hydrolysis by MKP3 in the presence of increasing concentrations of either wild-type or L4A H176E ERK (as described in the Materials and Methods). As is evident from Figure 6A,B, the L4A H176E ERK mutant displayed binding/activation curves that were indistinguishable (within error) from wild-type ERK. The calculated dissociation constants of binding wild-type or L4A H176E ERK to MKP3 were 0.27 ± 0.06 and 0.20 ± 0.07 μM, respectively (Figure 6A,B). Utilizing the fluorescence binding assay described in Figure 1, we determined a K_d of 0.15 ± 0.02 μM between L4A H176E ERK and MKP3. The K_d of 0.27 μM is in good agreement with the value of 0.21 μM obtained for wild-type ERK using the fluorescent anisotropy binding experiment described previously. There is also excellent agreement between K_d values 0.20 and 0.15 μM obtained with the L4A H176E ERK mutant using the activation-based assay and the fluorescent anisotropy binding assay, respectively. More importantly, similar dissociation constants for MKP3 binding to L4A H176E or wild-type ERK indicate that overall binding and activation of MKP3 are unaffected by these mutations. To test the ability of MKP3 to dephosphorylate the L4A H176E pERK, we compared the k_{cat}/K_m values with wild-type pERK and L4A H176E pERK as substrates. The k_{cat}/K_m value (0.88 ± 0.23 × 10^6) using L4A H176E pERK was only ~3-fold lower than that observed with wild-type pERK (3.1 ± 1.9 × 10^6) (Figure 6C,D). This similarity in k_{cat}/K_m values provides additional support that the monomeric form of pERK is the relevant substrate for MKP3. Together, our studies suggest that the heterodimer of MKP3 and phosphorylated ERK is the physiologically relevant complex.

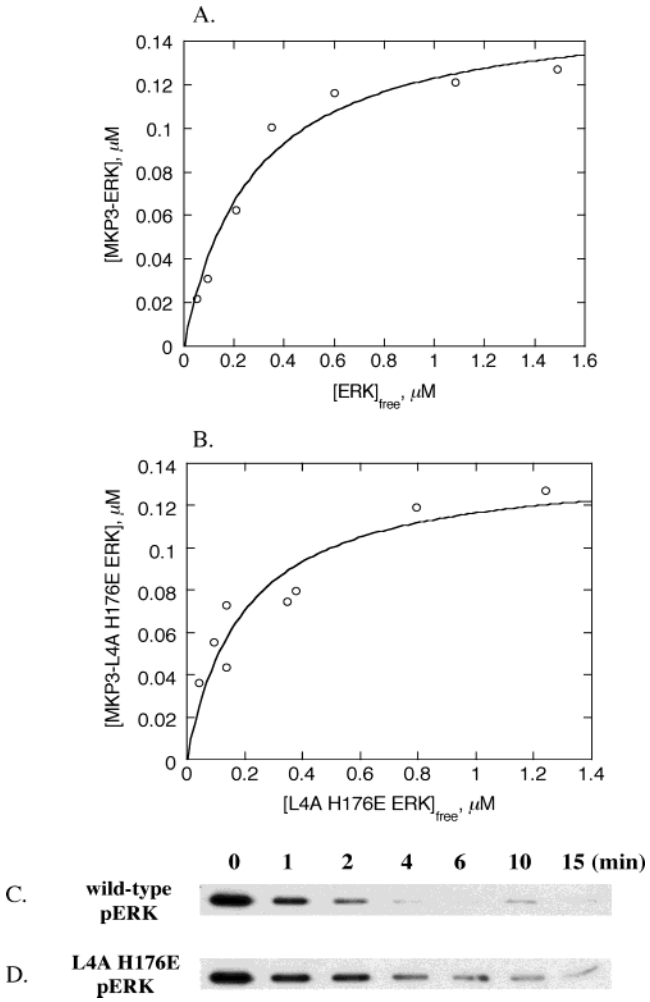

FIGURE 6: Dephosphorylation of wild-type and L4A H176E mutant pERK by MKP3. (A and B) Dissociation constants of wild-type ERK and L4A H176E ERK to MKP3. The *V*/*K* values for *p*NPP hydrolysis at different ERK protein concentrations were measured, and the concentration of MKP3-bound ERK was determined as outlined in the Materials and Methods. The bound ERK concentrations were plotted against free ERK concentration, and the data were fitted to eq 4 to obtain the dissociation constant. Dissociation constants of wild-type ERK and L4A H176E ERK to MKP3 were 0.27 ± 0.06 and 0.20 ± 0.07 μM, respectively. These values are an average of three separate experiments. (C and D) Dephosphorylation of wild-type and L4A H176E mutant pERK by MKP3. Recombinant wild-type and L4A H176E mutant pERK at a final concentration of 1 μM were combined with 0.14 μM recombinant wild-type MKP3 in TBA, pH 7.0 at 25 °C. The rate of dephosphorylation was measured using the integrated Michaelis−Menten equation including an inhibition constant term K_i (eq 3). *V*/*K* for wild-type pERK dephosphorylation was (3.1 ± 1.9) × 10^6 M^{-1} s^{-1} and that for the L4A H176E pERK dephosphorylation was (0.88 ± 0.23) × 10^6 M^{-1} s^{-1}. These values are an average of three separate experiments.

DISCUSSION

In addition to its role in mediating catalytic activation of the carboxy terminus, we have demonstrated that the N-terminal domain of MKP3 mediates intramolecular dephosphorylation between the monomeric form of phosphorylated ERK and a monomer of MKP3 (Figure 7). Thus, monomeric pERK binds to the N-terminal domain of MKP3 and is dephosphorylated by the same molecule of MKP3. By tethering pERK to the N-terminal domain of MKP3, the C-terminal catalytic domain enjoys an increase in effective substrate concentration. Using the MKP3/VHR chimera protein (Table 1 and Figure 2) to estimate this catalytic advantage, the increased effective concentration contributes about ~40-fold to the k_{cat}/K_m value. This is probably a lower estimate given the potential suboptimal substrate orientation of the chimera relative to MKP3. Binding of ERK to MKP3 also induces catalytic activation, which contributes ~100-fold rate acceleration in the k_{cat}/K_m value (*16*, *20*, *21*). Even ignoring the basic contribution of the initial tight binding affinity (K_d ≤210 nM) between ERK and MKP3, the intramolecular dephosphorylation mechanism creates a reaction that is ~4000-fold more efficient toward its target

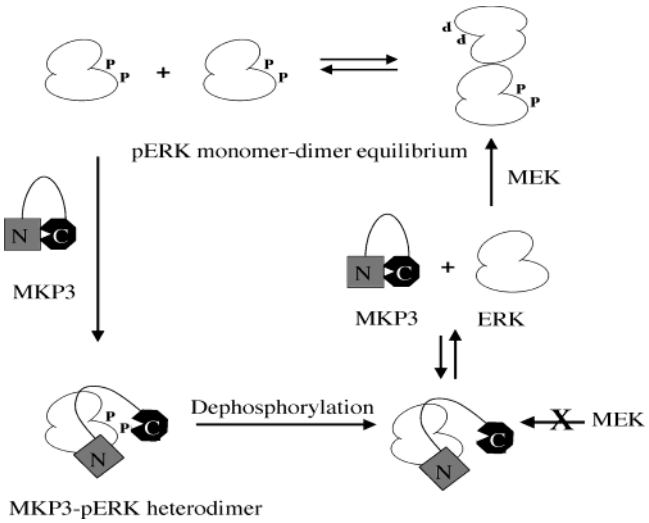

FIGURE 7: Proposed model for pERK down-regulation involving the formation of a MKP3-pERK heterodimer and intramolecular dephosphorylation. Details of this model are discussed in the text.

substrate. MKP3 is an exquisite example of both regulated and specific catalysis, creating a virtual magic bullet toward pERK.

Our general model for pERK dephosphorylation by MKP3 is depicted in Figure 7. Several additional insights can be gleaned from this model. It has been shown that ERK exists in a monomer−dimer equilibrium (*29*), which can be shifted toward dimer formation when ERK is phosphorylated by MEK. The crystallographic model of pERK was solved as a dimer (*44*). Consistent with these observations, our data indicate that pERK is (minimally) in a monomer−dimer equilibrium state. Dimerization of pERK is thought to provide the molecular switch that allows dimeric pERK to translocate from the cytosol to the nucleus (*29*). Here, cross-linking studies along with other presented data are entirely consistent with a simple heterodimeric complex between pERK monomer and MKP3 and provide strong evidence for the heterodimer as the functionally relevant Michaelis complex. However, we cannot rule out the possibility that MKP3 can bind and dephosphorylate dimeric ERK. Future studies will be directed at exploring this possibility. When pERK and MKP3 are present at equal-molar concentrations, monomeric MKP3 complexes with pERK (i.e., little of the monomer remains) to generate a species that is almost exclusively the heterodimer. Together, these data suggest that the binding between pERK and MKP3 is tighter than the binding between pERK monomers and that binding may be mutually exclusive. Although for technical reasons we were unable to measure a K_d value between pERK and MKP3 (C293S), Zhao et al. have reported a Michaelis constant K_m of 0.022 ± 0.005 μM (*23*). Khokhlatchev et al. (*29*) have reported a K_d value of 7.5 nM for pERK dimerization. Given the significant amount of pERK monomer reported by Khokhlatchev et al. (*29*) in the latter study, we believe the K_d value from equilibrium sedimentation data may be a high estimate of the actual binding affinity between pERK monomers (*29*). Our data are consistent with the idea that MKP3 binding to pERK or ERK may prevent the ability of ERK to dimerize. We have used molecular modeling of the available X-ray/NMR structures of VHR (*43*), pERK (*44*), the N-terminal domain of MKP3 (*33*), and the C-terminal domain of MKP3 (*45*) to examine the idea of mutually exclusive binding. The N-terminal noncatalytic domain and the C-terminal catalytic domain of MKP3 were solved separately. The structure of the linker region (~50 amino acid residues) between two domains has not been solved. Using the VHR−phosphopeptide structure (*43*) as a guide, we oriented the catalytic domain of MKP3 (*33*) onto a monomer of pERK (*44*). The location of the N-terminal domain binding site on pERK was modeled, in part, using the Arg residues (Arg 64/65) in the N-terminal domain of MKP3, which were shown to be important in interacting with ERK (*35*, *45*), through Asp residues (Asp 316/319) located on the opposite face of the TxY phosphorylation motif (*22*). When the two domains of MKP3 and the pERK monomer were docked as described previously, the catalytic domain of MKP3 interacts with one side of pERK (TxY motif), and the N-terminal domain of MKP3 interacts on the opposite side of pERK (via Asp 316/319). This interaction is schematically drawn in the bottom half of Figure 7. To connect the two domains of MKP3, the 50 unaccounted for amino acids in the linker could be predicted to traverse the dimerization domain of pERK, preventing homodimerization, although the N-terminal domain and not the linker region may be involved in mutually exclusive binding. Future investigations will examine the idea of mutually exclusive binding and whether MKP3 can bind and dephosphorylate a covalently fused ERK dimer. If mutually exclusive binding is established, then additional studies will address whether the linker region, the N-terminal domain alone, or both regions are required to prevent ERK homodimerization.

The formation of a heterodimeric complex of MKP3 and ERK has several important implications in the regulation of ERK function, as well as nuclear translocation. There are three different postulated mechanisms for nuclear import of MAP kinase: passive diffusion of monomer, active transport of a homodimer, and nuclear pore complex-mediated, cytosol-independent transport (*37*, *39*, *46*). Formation of a heterodimer between MKP3 and pERK in the cytoplasm might prevent pERK translocating to the nucleus by anchoring pERK in the cytoplasm. Interestingly, this mode of regulation does not require MKP3 to be active as a phosphatase. Indeed, Brunet et al. showed that overexpression of an inactive form of MKP3 (C293S MKP3) could sequester ERK in the cytoplasm (*47*). Similarly, it has been shown that MEK anchors unphosphorylated ERK in the cytoplasm (*48*−*50*). The localization and the function of ERK may be ultimately determined by which protein(s) are associated (*37*, *39*, *51*). Tanoue et al. suggested that there is a docking domain in MAP kinases common to substrates, activators, and regulators, including MEK1, MNK1, and MKP3 (*22*). Others proposed that conserved docking sites in MEKs and substrate proteins mediate high affinity binding to MAP kinases (*52*−*54*). Using short synthetic peptides, recent studies by Bardwell et al. provided evidence that the regulators of ERK such as MEK1/2, Elk-1, and MKP1/2 bind to an overlapping region in ERK (*55*). Studies by Zhang et al. showed mutually exclusive binding of MKP3 and MEK to ERK using GST pull-down assays (*56*). Together, these studies support a model where the formation of a heterodimer between MKP3 and ERK might prevent further activation of ERK by blocking the binding site for MEK (Figure 7). Consistent with this idea, we have observed that unphos-

phorylated ERK bound to C293S MKP3 is highly resistant to phosphorylation by active MEK (Denu et al., unpublished observation). Thus, MKP3 not only downregulates pERK function by substrate-activated, intramolecular dephosphorylation but may also prevent pERK homodimerization and further activation by its upstream kinase MEK. However, it should be noted that Brunet et al., using a transient transfection system, concluded that inactive MKP3 (C293S) blocks MAPK nuclear translocation without affecting its phosphorylation by MEK (*47*). Although this contradictory observation may have resulted from the use of an artificially high activation of the MEK pathway, additional studies are needed to explore this potential mode of regulation.

This paper provides a framework for understanding the general and specific mechanisms employed by the MKP family of enzymes that regulate MAP kinases. The MKPs share similar structural domains consisting of the N-terminal noncatalytic domain and C-terminal catalytic domain. Given the observed specificity (*12*, *13*, *17*, *18*, *57*) and the catalytic activation seen with other MKPs (*17*, *19*, *20*, *21*, *32*, *58*), many of the reaction and regulatory mechanisms described here for MKP3 may be a general feature of other MKPs. Future work focusing on protein complex formation among and between the MKPs and the MAP kinases will provide additional insight into the exquisite regulation of these enzymes.

ACKNOWLEDGMENT

We thank Johanna Rigas for generating the antibody against MKP3, Melanie Cobb (University of Texas Southwestern) for providing the pGEX-KG H176E L_4A ERK2 Plasmid, and Jeffrey Hansen and Virgil Schirf (University of Texas Health Sciences Center) for performing the sedimentation velocity analysis.

SUPPORTING INFORMATION AVAILABLE

Supporting Information includes four figures showing that fluorescein labeling of ERK proteins has no significant effect on the ability to bind and activate MKP3, time-dependent dephosphorylation of pERK by VHR, and the MKP3/VHR chimera using a radioactive kinase assay; glutaraldehyde cross-linking of MKP3, ERK, and the mixture of MKP3 and ERK; and mobility differences in cross-linked species on SDS−PAGE involving ERK-MKP3, pERK−pERK, and ERK−pERK. This material is available free of charge via the Internet at http://pubs.acs.org.

REFERENCES

1. Pearson, G., Robinson, F., Beers Gibson, T., Xu, B. E., Karandikar, M., Berman, K., and Cobb, M. H. (2001) *Endocr. Rev. 22*, 153−83.
2. Johnson, G. L., and Lapadat, R. (2002) *Science 298*, 1911−2.
3. Pouyssegur, J., Volmat, V., and Lenormand, P. (2002) *Biochem. Pharmacol. 64*, 755−63.
4. Khokhlatchev, A., Xu, S., English, J., Wu, P., Schaefer, E., and Cobb, M. H. (1997) *J. Biol. Chem. 272*, 11057−62.
5. Groom, L. A., Sneddon, A. A., Alessi, D. R., Dowd, S., and Keyse, S. M. (1996) *EMBO J. 15*, 3621−32.
6. Sun, H., Charles, C. H., Lau, L. F., and Tonks, N. K. (1993) *Cell 75*, 487−93.
7. Ward, Y., Gupta, S., Jensen, P., Wartmann, M., Davis, R. J., and Kelly, K. (1994) *Nature 367*, 651−4.
8. Kwak, S. P., and Dixon, J. E. (1995) *J. Biol. Chem. 270*, 1156−60.
9. Keyse, S. M. (2000) *Curr. Opin. Cell Biol. 12*, 186−92.
10. Camps, M., Nichols, A., and Arkinstall, S. (1999) *FASEB J. 14*, 6−16.
11. Keyse, S. M., and Ginsburg, M. (1993) *Trends Biochem. Sci. 18*, 377−8.
12. Muda, M., Theodosiou, A., Rodrigues, N., Boschert, U., Camps, M., Gillieron, C., Davies, K., Ashworth, A., and Arkinstall, S. (1996) *J. Biol. Chem. 271*, 27205−8.
13. Chu, Y., Solski, P. A., Khosravi-Far, R., Der, C. J., and Kelly, K. (1996) *J. Biol. Chem. 271*, 6497−501.
14. Hirsch, D. D., and Stork, P. J. (1997) *J. Biol. Chem. 272*, 4568−75.
15. Zama, T., Aoki, R., Kamimoto, T., Inoue, K., Ikeda, Y., and Hagiwara, M. (2002) *J. Biol. Chem. 277*, 23909−18.
16. Camps, M., Chabert, C., Muda, M., Boschert, U., Gillieron, C., and Arkinstall, S. (1998) *FEBS Lett. 425*, 271−6.
17. Dowd, S., Sneddon, A. A., and Keyse, S. M. (1998) *J. Cell Sci. 111*, 3389−99.
18. Slack, D. N., Seternes, O. M., Gabrielsen, M., and Keyse, S. M. (2001) *J. Biol. Chem. 276*, 16491−500.
19. Hutter, D., Chen, P., Barnes, J., and Liu, Y. (2000) *Biochem. J. 352*, 155−63.
20. Fjeld, C. C., Rice, A. E., Kim, Y., Gee, K. R., and Denu, J. M. (2000) *J. Biol. Chem. 275*, 6749−57.
21. Zhou, B., and Zhang, Z. Y. (1999) *J. Biol. Chem. 274*, 35526−34.
22. Tanoue, T., Adachi, M., Moriguchi, T., and Nishida, E. (2000) *Nat. Cell Biol. 2*, 110−6.
23. Zhao, Y., and Zhang, Z. Y. (2001) *J. Biol. Chem. 276*, 32382−91.
24. Wiland, A. M., Denu, J. M., Mourey, R. J., and Dixon, J. E. (1996) *J. Biol. Chem. 271*, 33486−92.
25. Denu, J. M., Zhou, G., Wu, L., Zhao, R., Yuvaniyama, J., Saper, M. A., and Dixon, J. E. (1995) *J. Biol. Chem. 270*, 3796−803.
26. Robbins, D. J., Zhen, E., Cheng, M., Xu, S., Ebert, D., and Cobb, M. H. (1994) *Adv. Cancer Res. 63*, 93−116.
27. Yuvaniyama, J., Denu, J. M., Dixon, J. E., and Saper, M. A. (1996) *Science 272*, 1328−31.
28. Denu, J. M., Zhou, G., Wu, L., Zhao, R., Yuvaniyama, J., Saper, M. A., and Dixon, J. E. (1995) *J. Biol. Chem. 270*, 3796−803.
29. Khokhlatchev, A. V., Canagarajah, B., Wilsbacher, J., Robinson, M., Atkinson, M., Goldsmith, E., and Cobb, M. H. (1998) *Cell 93*, 605−15.
30. Wilsbacher, J. L., and Cobb, M. H. (2001) *Methods Enzymol. 332*, 387−400.
31. Todd, J. L., Tanner, K. G., and Denu, J. M. (1999) *J. Biol. Chem. 274*, 13271−80.
32. Camps, M., Nichols, A., Gillieron, C., Antonsson, B., Muda, M., Chabert, C., Boschert, U., and Arkinstall, S. (1998) *Science 280*, 1262−5.
33. Stewart, A. E., Dowd, S., Keyse, S. M., and McDonald, N. Q. (1999) *Nat. Struct. Biol. 6*, 174−81.
34. Alonso, A., Saxena, M., Williams, S., and Mustelin, T. (2001) *J. Biol. Chem. 276*, 4766−71.
35. Zhou, B., Wu, L., Shen, K., Zhang, J., Lawrence, D. S., and Zhang, Z. Y. (2001) *J. Biol. Chem. 276*, 6506−15.
36. Brunner, D., Oellers, N., Szabad, J., Biggs, W. H., III, Zipursky, S. L., and Hafen, E. (1994) *Cell 76*, 875−88.
37. Adachi, M., Fukuda, M., and Nishida, E. (1999) *EMBO J. 18*, 5347−58.
38. Matsubayashi, Y., Fukuda, M., and Nishida, E. (2001) *J. Biol. Chem. 276*, 41755−60.
39. Wolf, I., Rubinfeld, H., Yoon, S., Marmor, G., Hanoch, T., and Seger, R. (2001) *J. Biol. Chem. 276*, 24490−7.
40. Jia, Z., Barford, D., Flint, A. J., and Tonks, N. K. (1995) *Science 268*, 1754−8.
41. Flint, A. J., Tiganis, T., Barford, D., and Tonks, N. K. (1997) *Proc. Natl. Acad. Sci. U.S.A. 94*, 1680−5.
42. Garton, A. J., Flint, A. J., and Tonks, N. K. (1996) *Mol. Cell Biol. 16*, 6408−18.
43. Schumacher, M. A., Todd, J. L., Rice, A. E., Tanner, K. G., and Denu, J. M. (2002) *Biochemistry 41*, 3009−17.
44. Canagarajah, B. J., Khokhlatchev, A., Cobb, M. H., and Goldsmith, E. J. (1997) *Cell 90*, 859−69.
45. Farooq, A., Chaturvedi, G., Mujtaba, S., Plotnikova, O., Zeng, L., Dhalluin, C., Ashton, R., and Zhou, M. M. (2001) *Mol. Cell 7*, 387−99.

46. Whitehurst, A. W., Wilsbacher, J. L., You, Y., Luby-Phelps, K., Moore, M. S., and Cobb, M. H. (2002) *Proc. Natl. Acad. Sci. U.S.A. 99*, 7496−501.
47. Brunet, A., Roux, D., Lenormand, P., Dowd, S., Keyse, S., and Pouyssegur, J. (1999) *EMBO J. 18*, 664−74.
48. Volmat, V., Camps, M., Arkinstall, S., Pouyssegur, J., and Lenormand, P. (2001) *J. Cell Sci. 114*, 3433−43.
49. Rubinfeld, H., Hanoch, T., and Seger, R. (1999) *J. Biol. Chem. 274*, 30349−52.
50. Adachi, M., Fukuda, M., and Nishida, E. (2000) *J. Cell Biol. 148*, 849−56.
51. Schmidt, C., Pommerenke, H., Durr, F., Nebe, B., and Rychly, J. (1998) *J. Biol. Chem. 273*, 5081−5.
52. Bardwell, A. J., Flatauer, L. J., Matsukuma, K., Thorner, J., and Bardwell, L. (2001) *J. Biol. Chem. 276*, 10374−86.
53. Xu, B., Stippec, S., Robinson, F. L., and Cobb, M. H. (2001) *J. Biol. Chem. 276*, 26509−15.
54. Fantz, D. A., Jacobs, D., Glossip, D., and Kornfeld, K. (2001) *J. Biol. Chem. 276*, 27256−65.
55. Bardwell, A. J., Abdollahi, M., and Bardwell, L. (2003) *Biochem. J. 370*, 1077−85.
56. Zhang, J., Zhou, B., Zheng, C.-F., and Zhang, Z. Y. (2003) *J. Biol. Chem. 278*, 29901−12.
57. Muda, M., Boschert, U., Smith, A., Antonsson, B., Gillieron, C., Chabert, C., Camps, M., Martinou, I., Ashworth, A., and Arkinstall, S. (1997) *J. Biol. Chem. 272*, 5141−51.
58. Slack, D. N., Seternes, O. M., Gabrielsen, M., and Keyse, S. M. (2001) *J. Biol. Chem. 276*, 16491−500.

BI035346B